Analytical Methods

PAPER

View Article Online
View Journal | View Issue

Cite this: *Anal. Methods*, 2014, **6**, 521

On the applicability of $SiO_2/Al_2O_3/Nb_2O_5$ and $SiO_2/Al_2O_3/TiO_2$ as a biocompatible platform for chloroperoxidase

Márcia Simões Ribeiro,[a] Fábio Jorge de Vasconcellos Júnior,[a] Bruna Teixeira da Fonseca,[a] Flávia Carvalho de Souza,[ab] Felipo Doval Rojas Soares,[a] Éder Cláudio Lima,[c] Murilo Feitosa Cabral,[d] Emerson Schwingel Ribeiro[a] and Eliane D'Elia*[a]

Received 26th August 2013
Accepted 28th October 2013

DOI: 10.1039/c3ay41468j

www.rsc.org/methods

In the present work, two mixed oxides, namely, $SiO_2/Al_2O_3/Nb_2O_5$ and $SiO_2/Al_2O_3/TiO_2$ (designated as SiAlNb and SiAlTi, respectively), obtained using the sol–gel method were used to immobilize chloroperoxidase. Hydrogen peroxide was quantified using potassium hexacyanoferrate(II) as a redox-mediator and amperometric measurements at 0.0 V *vs.* Ag/AgCl/Cl^- (3 M). The SiAlTi biosensor presented higher sensitivity than the SiAlNb biosensor, however, the first one did not present a good response regarding time. The developed biosensor using the SiAlNb mixed oxide provided good signal levels, good linearity, good stability (retaining approximately 70% of its original response after 6 weeks of usage), a low detection limit (3 μM), good sensitivity, a suitable working range (from 4 to 19 μM), fast response and good repeatability. The recovery of the amperometric method for the detection of hydrogen peroxide in synthetic samples was approximately 100 ± 2%, and for Listerine® Whitening Pre-Brush Rinse samples fortified with 1, 2 and 3% (v/v) of hydrogen peroxide, it was 100 ± 3%.

Introduction

Recently, many support materials, such as Nafion, silica sol–gel, chitosan (CS) and poly(vinyl alcohol), have been used for immobilizing enzymes.[1–6] Among these materials, the mixed oxides are promising for the development of biosensors. In this way, the long-term stability of biomolecules attached on inorganic matrixes has been an interesting subject matter.

Inorganic matrixes have shown useful physical–chemical properties, such as morphology, biocompatibility and chemical composition. Many kinds of sol–gel based materials have been applied for both covalent and physical adsorption immobilization of biomolecules (*e.g.*, Enzymes). As a great advantage, these materials (*i.e.*, Titania,[7] $NiFe_2O_4$/CuO/FeO–chitosan,[8] SiO_2[9] and TiO_2–CeO_2 [10]) have shown biocompatible features, which they are able to keep their properties after the immobilization procedure.

The preparation of SiO_2/M_xO_y or $SiO_2/M_xO_y/M_xO_y$ oxides obtained by the sol–gel process combines the mechanical properties of the silica matrix with the chemical properties of the bulk metal oxides (M_xO_y). The sol–gel process also enables a solid with controlled porosity to be obtained, and the metal oxide can be obtained as highly dispersed particles in the silica matrix. Basically, this procedure consists of the reaction between tetraethyl orthosilicate and the metal oxide precursor.

The SiO_2/M_xO_y materials have found use in many applications,[11–25] such as their use as a porous substrate to immobilize electroactive species to prepare chemically modified electrodes.[11–14] The metal oxides (such as SnO_2, TiO_2, Sb_2O_5 and Nb_2O_5) are dispersed in the silica matrix, and they present acidic and basic properties, which enables them to be used for adsorbing enzymes.

Several authors have reported that adsorption and/or covalent entrapment can provide a simple way to immobilize a variety of proteins to sol–gel based materials.[26–36]

Among other enzymes that can be used as a model to study interactions with sol–gel based materials, chloroperoxidase (CPO) offers useful features. Besides its wide applicability to the detection and quantification of peroxide, a common target, CPO is a versatile heme-containing enzyme that exhibits peroxidase, catalase and cytochrome P450-like activities in addition to catalyzing halogenation and H_2O_2 decomposition reactions.[37] For that reason, this enzyme can be used as a model to investigate the interaction of CPO with a variety of inorganic and organic matrixes, commonly used in the development of biosensors.[38–41]

Our group recently demonstrated the use of the SiAlNb and SiAlTi for the pre-concentration of metal ions in solution[42–44] and also, the use of the SiAlNb in development of electrochemical

[a]*Instituto de Química, Universidade Federal do Rio de Janeiro (UFRJ), Rio de Janeiro, RJ, CEP 21941-909, Brazil. E-mail: eliane@iq.ufrj.br*

[b]*Intituto Federal do Rio de Janeiro - Campus São Gonçalo, São Gonçalo, RJ, CEP 24425-005, Brazil*

[c]*Instituto de Química, Universidade Federal do Rio Grande do Sul (UFRGS), Porto Alegre, RS, CEP 91501-970, Brazil*

[d]*Instituto de Química de São Carlos/USP, Departamento de Físico-Química, São Carlos, SP, CEP 13560-970, Brazil*

biosensors for amitriptyline and promethazine determinations.[45,46] Additionally, Yoshida and co-workers reported that the $SiO_2/Al_2O_3/TiO_2$ oxide exhibited high photocatalytic activity in the photoinduced direct methane coupling to produce H_2 and ethane.[47] Crisan and co-workers demonstrated that $Al_2O_3/TiO_2/SiO_2$ had a high reactivity, and the formation of tialite was improved.[48] $Al_2O_3/SiO_2/TiO_2$ nanocomposites loaded with vanadium demonstrated the selective catalytic reduction of NO_x using ammonia as a reductant.[49] This ternary material has been prepared by other authors.[50,51] However, the use of SiAlNb and SiAlTi as a biocompatible platform for chloroperoxidase to prepare modified electrodes has not been described in the literature, despite the great potential of these materials.

Aiming to understand and characterize the properties of SiAlNb and SiAlTi, before and after the attachment of CPO through adsorption technique, this paper describes results obtained by a combination of physical and electrochemical measurements. Experimental results are complemented with further analysis by statistical treatment of electrochemical data.

Experimental

Synthesis of $SiO_2/Al_2O_3/Nb_2O_5$ and $SiO_2/Al_2O_3/TiO_2$

$SiO_2/Al_2O_3/Nb_2O_5$, which was designated as SiAlNb, was prepared according to a previously described procedure with several modifications.[43,44] Specifically, 13 mL of a 3.5 M solution of HCl was added to 230.0 mL of a 50% (v/v) solution of ethanol/TEOS. The mixture was stirred for 3 h at 70 °C. After the pre-hydrolysis step, 20.5 g of aluminium isopropoxide (dissolved in a small amount of trifluoroacetic acid) and 10.3 g of $NbCl_5$ (previously dissolved in ethanol under a nitrogen atmosphere) were added, and the resulting mixture was stirred for 20 h at 70 °C. The solvent was slowly evaporated at 80 °C until a gel has formed and was subsequently heated for 4 h in an oven at 80 °C. The obtained gel was ground and dried under vacuum (1.3×10^{-2} Pa) for 4 h. Subsequently, the resulting particles were washed with ethanol in a Soxhlet extractor for 6 h. Finally, the particles were dried under vacuum (1.3×10^{-2} Pa) for 2 h at 80 °C and were stored.

$SiO_2/Al_2O_3/TiO_2$, which was designated as SiAlTi, was prepared according to a previously described procedure with several modifications.[42] 13.0 mL of a 3.5 M solution of HCl was added to 230.0 mL of a 50% (v/v) solution of ethanol/TEOS. The mixture was stirred for 3 h at 70 °C. After the pre-hydrolysis step, 66.0 mL of titanium(IV) butoxide and 15.0 mL of 3.5 M HCl were added. The mixture was stirred for 2 h at 70 °C. Next, 11.0 g of aluminium isopropoxide (dissolved in 5 mL of trifluoroacetic acid) was added, and the resulting mixture was stirred for 20 h at 70 °C. The solvent was slowly evaporated at 70 °C until the gel formed and was later heated for 4 h in an oven at 70 °C. The final product was carefully crushed, and the remaining solvent was evaporated at 70 °C under vacuum (1.3×10^{-2} Pa) for approximately 4 h, which resulted in a completely dry gel. The resulting material was ground in a mortar, sieved and washed in a Soxhlet extractor for 6 h with ethanol followed by 100.0 mL of 0.1 M HNO_3; next, the material was washed repeatedly with ethanol, deionised water and with ethanol again. Finally, the solid was dried at 60 °C under vacuum (1.3×10^{-2} Pa) for approximately 2 h at room temperature and was stored.

Reagents and solutions

HEPES buffer, chloroperoxidase from Caldariomyces fumago (CPO) 38 200 units mL^{-1}, glutaraldehyde solution (25%), tetraethylorthosilicate (TEOS) (98% v/v), $NbCl_5$ (99% w/w), titaniumbutoxide (97% v/v), aluminium isopropoxide (98% w/w) and trifluoroacetic acid (99% v/v) were purchased from Sigma-Aldrich (Saint Louis, MO, USA), ethanol solution from Vetec (Duque de Caxias, RJ, Brazil), H_2O_2 (30% w/v) and potassium hexacyanoferrate(II) from Merck (Darmstadt, Germany), graphite 99.9% grade from Fluka (Buchs, Switzerland) and hydrocarbon oil from a commercial source. All solutions were prepared using ultra-pure water (>18.2 MΩ cm^{-1}, Milli-Q Millipore, Billerica, MA, USA).

Biosensor preparation

The immobilization of the enzyme on the surface of the mixed oxide was performed by adding of 800 μL of a chloroperoxidase solution (1.5 mg mL^{-1}) to 60 mg of the mixed oxide (SiAlNb or SiAlTi) with 180 μL of a 0.1 M HEPES buffer (pH 7) and 20 μL of a 5% glutaraldehyde aqueous solution. The mixture was allowed to react at 14 °C for 30 min for simple adsorption and dried with nitrogen. The mixed oxide modified carbon paste electrode was prepared by mixing 60 mg of graphite, 40 mg of the material containing the immobilized enzyme and a drop of hydrocarbon oil as the binder. The newly prepared materials were named as CPO/SiAlNb/C and CPO/SiAlTi/C.

Electrochemical measurements

All of the electrochemical measurements were performed at 25 °C in a three-electrode cell with a 30 mL capacity. The cell was placed in a Faraday cage to avoid electrical noise. The electrochemical cell has a Teflon® cover that hosts the mixed oxide modified carbon paste electrode with immobilized CPO as the working electrode (geometric area *ca.* 0.20 cm^2), Ag/AgCl/KCl (3 M) as the reference electrode and platinum wire with a high surface area as the counter electrode, and degassing procedures were performed under a pure nitrogen atmosphere. All of the measurements were performed using a potentiostat/galvanostat (Micro Autolab from Eco-chemie) controlled by the GPES 4.8 software package.

The electrochemical characterization of the biosensors using CPO/SiAlNb/C and CPO/SiAlTi/C was performed by cyclic voltammetry with a scan rate of 10 mV s^{-1} in 0.1 M of a phosphate buffer (pH 7.2) in the absence and presence of potassium hexacyanoferrate(II) solely and with addition of hydrogen peroxide. The amperometric response of the biosensor for the detection of H_2O_2 was performed at 0.0 V for 30 s. The supporting electrolyte solution used was a mixture that contained 0.1 M phosphate buffer (pH 7.2) and 0.1 M of potassium hexacyanoferrate(II) as a redox-mediator.

The analytical curves were constructed by adding aliquots of a standard solution of hydrogen peroxide to the electrochemical cell, which ranged in concentration from 4 to 19 μM of

hydrogen peroxide in 15 mL of the supporting electrolyte solution. The analysis was performed in triplicate for each concentration. For each measurement, the solution contained in the electrochemical cell was mixed by magnetic agitation for 20 s to obtain a homogeneous solution and to allow the catalysis of peroxide by CPO.

The analytical performance of the chronoamperometric method for the quantitative determination of hydrogen peroxide using the biosensor was performed using several basic determinations, such as the linearity, detection and quantification limits, recovery and precision.

The detection limits (DL) for the chronoamperometric method were obtained from the experimental data based on three statistical criteria: the $3.3\sigma_c/b$, $3\sigma_b/b$ and $3\sigma_b + X_b$, where b is the slope of the linear analytical curve, σ_c is an estimate of the standard deviation of the analytical curve, σ_b is an estimate of the standard deviation of the blank samples and X_b is the average value for a blank sample. Ten blank samples were analyzed to determine the detection limits. Grubb's test was used to check for possible outliers, and all measurements fell within a 95% confidence interval.[52,53]

For the linearity study, the analytical curve was obtained using a linear regression model to fit the data of current difference *versus* the known concentration of the hydrogen peroxide standard, which ranged from 4 to 19 μM.

These curve data were submitted to the Cochran test to determine whether the bilateral deviation of the variances was significant (5% or less). Plots of the residuals were obtained from the differences between the concentration values calculated from the linear regression line and the values obtained experimentally for evaluating the homoscedasticity. The precision of the method was statistically evaluated by observing the standard deviation of several analyses (repeatability).

The recovery study for this method was performed using synthetic samples of hydrogen peroxide ranging in concentration from 4 to 19 μM in the supporting electrolyte solution, and the samples recovery study was performed after fortifying a commercial tooth cleaning solution with 1, 2 and 3% (v/v) of hydrogen peroxide, which are concentrations close to the hydrogen peroxide content in the original sample.

Instrumentation

The Al_2O_3, Nb_2O_5 and TiO_2 contents in the materials were determined using energy-dispersive X-ray fluorescence analysis (EDFRX) on a model 800 HS EDX from Shimadzu (Tokyo, Japan).

The analysis of the specific surface area (S_{BET}) of the materials were performed on a Quantachrome Model Nova 1200e (Boynton Beach, Florida, USA) instrument and determined using the BET (Brunauer, Emmett and Teller) multipoint method by submitting the samples to previous activation at 250 °C in vacuum for 4 h. The BJH method was used to obtain the average pore size and the average pore volume.

For the scanning electron micrographs (SEM) and electron dispersive spectroscopy (EDS) analyses, the sample was dispersed on double-sided conductive tape on a copper support and coated with gold before the experiment. SEM images were acquired using a JEOL model JSM 6360-LV scanning electron microscope at an acceleration voltage of 20.0 kV (Tokyo, Jeol, www.jeol.co.jp) and 330× magnification.

Results and discussion

Characterization of SiAlNb and SiAlTi

By means of EDFRX, the initial amounts of the precursors used in the synthetic routes should yield materials with 20.0 wt% of Al_2O_3 and 20.0 wt% of Nb_2O_5 in the SiAlNb and 10.0 wt% of Al_2O_3 and 30.0 wt% of TiO_2 in the SiAlTi. However, the results from EDFRX analyses revealed that approximately 19.9 wt% of Al_2O_3 and 20.9 wt% of Nb_2O_5 were incorporated in SiAlNb, and 9.8 wt% of Al_2O_3 and 30.3 wt% of TiO_2 in SiAlTi; these values are close to the theoretical values. It is also worth mentioning that the hydrolysis process is not effective in the reaction media for all of the precursors. In this way, it is difficult to obtain mixed oxides using the sol–gel method with three different components in the desired proportions. However, this method is extremely useful for the synthesis of the materials.

The BET analyses revealed that the specific surface area of SiAlNb was 306 $m^2\ g^{-1}$ and of SiAlTi was 437 $m^2\ g^{-1}$. The BJH method revealed an average pore size of 15.3 Å for SiAlNb and 15.0 Å for SiAlTi, which indicates that these materials are microporous, and the observed values for the average pore volume were 0.026 $cm^{-3}\ g^{-1}$ for SiAlNb and 0.036 $cm^{-3}\ g^{-1}$ for SiAlTi. These values are similar to those reported in literature for mixed oxides obtained using sol–gel processes.[42–44] Furthermore, these values reflect a good accessibility to active sites, which is a fundamental characteristic for the adsorption of enzymes.

Fig. 1 shows scanning electron images for a single particle of SiAlNb, the morphology was characterized by a flat surface with a rough structure and does not present uniform size and shape. These features can contribute to the enzyme physical

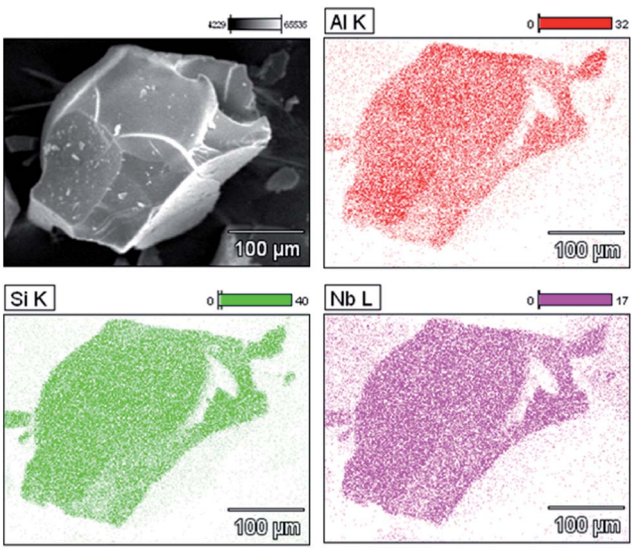

Fig. 1 Scanning electron micrograph of SiAlNb and the corresponding mapping of the Al (red), Si (green), and Nb (purple) elements by EDS. Magnification of 330×.

adsorption, since these defects figured out as good platform for the biological molecules. A typical energy dispersive scanning image (EDS) of the elements in the SiAlNb material is also shown in Fig. 1. The images suggest a good dispersion of the mixed oxides on the silica surface, and studied at this level, we can observe a homogeneous material without the formation of islands or phase segregation. This dispersion of the mixed oxides in the silica matrix is highly desirable because it increases the number of acidic sites on the surface of the material, which enhances its efficiency for the immobilization of enzymes. Furthermore, this high dispersion can be attributed to strong interactions with the siloxane groups of the silica surfaces by means of covalent bonds with other oxides in the material. The same characteristics are observed for SiAlTi (images not shown).

Electrochemical measurements

Fig. 2 depicts the cyclic voltammograms obtained from the biosensors using CPO/SiAlTi/C (Fig. 2A) and CPO/SiAlNb/C (Fig. 2B) in the presence and absence of $[Fe(CN)_6]^{4-}$ and hydrogen peroxide. We do not find any obvious electrochemical peaks in this potential range as the lack of electron mediator for CPO/SiAlNb/C. On the other hand the TiO_2 from CPO/SiAlTi/C presents redox behaviour with a small current response in this potential range. As can be seen from Fig. 2A and B, in the presence of $[Fe(CN)_6]^{4-}$ an increase of the electrochemical signal can be observed due to the reduction and oxidation of $[Fe(CN)_6]^{3-/4-}$, when compared with the blank signal (only PBS buffer). Upon addition of 15 μM H_2O_2 to electrolyte solution an electrocatalytical response was observed wherein both reduction and oxidation peak currents increased indicating good catalytic activity toward H_2O_2 and an effective CPO immobilization.

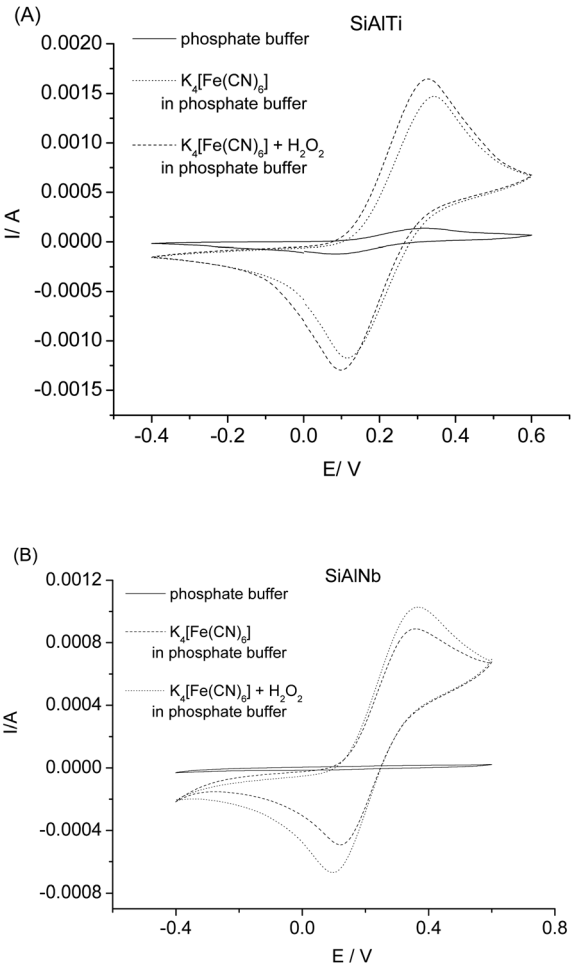

Fig. 2 Cyclic voltammograms of the SiAlNb and SiAlTi modified carbon paste electrodes with immobilized chloroperoxidase without H_2O_2 and with 15 μM H_2O_2 in phosphate buffer.

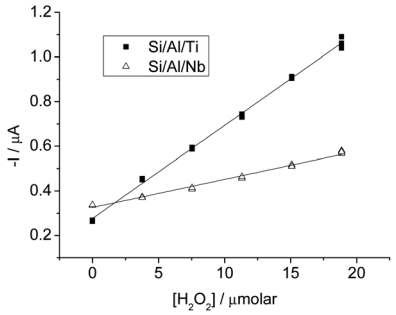

Fig. 3 Analytical curves obtained for both SiAlNb and SiAlTi modified carbon paste with immobilized CPO electrodes ($E = 0.0$ V).

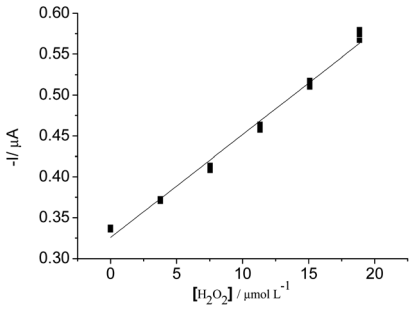

Fig. 4 Analytical curve of amperometric responses *vs.* hydrogen peroxide concentration.

The analytical curves obtained, with the biosensors using SiAlNb and SiAlTi modified carbon paste electrodes with immobilized chloroperoxidase are compared in Fig. 3. The parameters obtained from these analytical curves are the slope, linear coefficient, linear correlation coefficient and standard deviation curve, and they are presented in Table 1 for comparison.

The linear correlation coefficients revealed that the amperometric method using both biosensors has a linear correlation greater than 99%. Although the CPO/SiAlTi/C biosensor presented higher sensitivity than the CPO/SiAlNb/C biosensor, the standard deviation curve of the first one is also higher, which indicates a superior data dispersion of the linear fit. Furthermore, the CPO/SiAlTi/C biosensor did not present a good response with respect to time. The long-term stability of the biosensors was investigated by measuring the current response of 19 μM of H_2O_2 every other day over the course of 6 weeks. The

Table 1 Parameters obtained from the analytical curves shown in Fig. 3

Statistical parameters of curves	SiAlTi	SiAlNb
Slope (μA/μM)	0.0417	0.0125
Linear coefficient (μA)	0.2766	0.3257
Linear correlation coefficient	0.9987	0.9945
Standard deviation curve	0.0143	0.0090

Table 2 Detection and quantification limits for the chronoamperometric detection of hydrogen peroxide in solution

Criterion	DL (μM)	QL (μM)
Standard deviation curve ($3.3\sigma_c/b$)	2	6
Slope ($3\sigma_b/b$)	0.4	1.2
Standard deviation blank ($3\sigma_b + X_b$)	3	4
Experimental	3	9

results indicated that the response of the CPO/SiAlNb/C biosensor decreased by 4% of its initial current after 1 week and retained approximately 70% of its original response after 6 weeks of usage, whereas the CPO/SiAlTi/C biosensor lasted only one day. Looking for applicability of one of these materials in real sample analysis, we chose to work with the CPO/SiAlNb/C biosensor, since it showed better stability.

The biocatalytic performance of the CPO-mediated modified sol–gel based material was determined by amperometry measurements. Fig. 4 shows typical amperometric responses of a sensing biosensor poised at 0.0 V ($t = 30$ s). The increase in cathodic current can be observed with each addition of the hydrogen peroxide standard solution, indicative of the enhancement of reduction current by the catalytic reaction on the electrode surface. In fact, $[Fe(CN)_6]^{4-}$ plays as a mediator for CPO to recover its catalytic site. CPO is dependent of an electron donor to reduce H_2O_2. Therefore, the electrochemical signal observed is proportional to the amount of H_2O_2 reduced by CPO. Such behaviour is similar to that presented by peroxidase enzymes, *e.g.*, HPR.[54]

The curve presented in Fig. 4 has an excellent correlation coefficient ($r = 0.9945$). This graph indicates that the linear regression model was correct because the residues did not exceed 0.017 μA, which was close to the baseline noise (Fig. 5).

The Cochran test was applied to the amperometric method, and the calculated value (0.490) was also lower than the tabulated value (0.707) for the curve over the range from 4 to 19 μM. This result indicated homogeneous variances of the response with changing analyte concentration, which characterizes homoscedastic behaviour.

Statistical studies were used to determine the detection (DL) and quantification (QL) limits for the amperometric method using the SiAlNb biosensor. The calculated values for the detection and quantification limits of hydrogen peroxide were compared with the values obtained experimentally, as shown in Table 2. The statistically obtained detection and quantification limit values were similar to the experimental values of 3 and 9 μM, respectively.

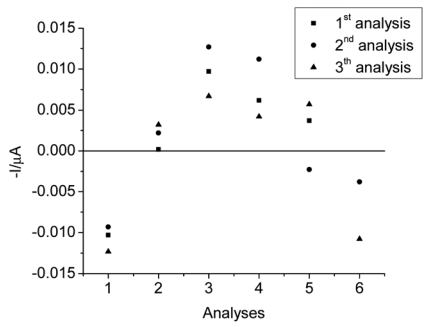

Fig. 5 Graph of residuals collected from the analytical curve obtained by the chronoamperometric method using the CPO/SiAlNb/C.

The precision of the amperometric method was evaluated for its repeatability by observing the standard deviation obtained for each concentration of analyte in the range from 4 to 19 μM. A good repeatability was verified (*i.e.*, there were only small variations in the results of the duplicate analyses performed within a short time using the same conditions). The relative standard deviation (RSD) values did not exceed 1.1% variability (see Table 3), which is considered acceptable for this type of technique and indicates a good precision for this type of analysis.

The recovery of the amperometric method for the detection of hydrogen peroxide in synthetic samples (in the range from 4 to 19 μM) was approximately 100 ± 2%, as observed in Table 3.

The commercial tooth cleaning solution sample was analyzed using the amperometric method with CPO/SiAlTi/C biosensor, and the hydrogen peroxide content was 1.98% (v/v), which is very close to the value provided by the manufacturer (2.0% (v/v)).[55]

The recovery for the detection of hydrogen peroxide in the commercial tooth cleaning solution sample fortified with 1, 2 and 3% (v/v) of hydrogen peroxide was 100 ± 3%, as shown in Table 4. These results indicate that there were no matrix effects in the hydrogen peroxide recovery in this type of sample.

Table 5 shows the performance of the CPO/SiAlNb/C modified electrode in comparison with other amperometric sensors based on carbon paste electrodes for the determination of hydrogen peroxide. As can be observed, the CPO/SiAlNb/C modified electrode presented good performance, showing the potentiality of the CPO/SiAlNb/C modified electrode as a sensor for hydrogen peroxide using mixed oxide synthesized by a simple low-cost novel route.

Conclusions

A sol–gel method was used to prepare two mixed oxides, SiAlTi and SiAlNb, which were used to immobilize chloroperoxidase and to prepare the modified carbon paste electrodes. Hydrogen peroxide was quantified using potassium hexacyanoferrate(II) as a redox-mediator and performing amperometric measurements at 0.0 V *vs.* Ag/AgCl/KCl (3 M).

Table 3 Data for the analytical curve obtained from different standard concentrations of hydrogen peroxide by the chronoamperometric method using the SiAlNb modified carbon paste electrode with immobilized CPO

Hydrogen peroxide concentration (μM)	1st signal (μA)	2nd signal (μA)	3nd signal (μA)	Average (μA)	S^2 $(\mu A)^2$	RSD (%)	Recovery (%)
0	0.336	0.335	0.338	0.336	2.3×10^{-6}	0.5%	103%
4	0.373	0.371	0.370	0.371	2.3×10^{-6}	0.4%	100%
7,5	0.411	0.408	0.414	0.411	9.0×10^{-6}	0.7%	98%
11	0.462	0.457	0.640	0.461	1.3×10^{-5}	0.8%	100%
15	0.512	0.518	0.510	0.513	1.7×10^{-5}	0.8%	100%
19	0.580	0.567	0.574	0.574	4.2×10^{-5}	1.1%	102%

Table 4 Recovery results obtained from the amperometric quantification of hydrogen peroxide added to the Listerine® Whitening Pre-Brush Rinse sample

Theoretical hydrogen peroxide concentration (%)	Measured iodide concentration (%)	Standard deviation	Variance	Recovery
1.0	1.02	0.03	0.001	102%
	1.02			102%
	0.96			96%
2.0	2.10	0.08	0.006	105%
	1.95			98%
	2.02			101%
3.0	2.95	0.04	0.002	98%
	3.03			101%
	2.99			100%

Table 5 Performance of the CPO/SiAlNb/C modified electrode in comparison with other amperometric sensors prepared in different solid supports for the determination of H_2O_2[a]

Electrode	Linear range/μM	Detection limit/μM	Quantification limit/μM	Sensitivity	Ref
CPO/SiAlNb/C	4.0–19.0	3.0	4.0	0.0125 μA μM^{-1}	This work
Hemoglobin immobilized at multiwalled carbon nanotubes–zinc oxide composite (WCNT/ZnO/Hb)	0.1–36.6	0.02	n.a.	3.66 μA μM^{-1}	56
HRP–nanogold–PTH–nanogold–CPE (HRP/Au/PTH/Au–CPE)	9.6–1200	0.75	n.a.	0.011 μA μM^{-1}	57
Cryptomelane-type manganese oxides modified CPE	100–690	2.0	n.a.	n.a.	58
Phosphomolybdate–polypyrrole composite	200–30 000	50.0	n.a.	1.1 μA mM^{-1}	59
Rhodium–Prussian blue modified carbon paste electrode (Rh–PBMCPE)	50–860	28.0	n.a.	1.32 A cm^{-2} M^{-1}	60

[a] n.a.: Not available.

The CPO/SiAlTi/C biosensor presented higher sensitivity for the detection of H_2O_2 than did the CPO/SiAlNb/C biosensor; however, the first sensor did not present a good response with respect to time. The developed biosensor using the CPO/SiAlNb/C mixed oxide provided good signal levels, good linearity, good stability, a low detection limit, good sensitivity, a suitable working range, fast response and good repeatability.

Acknowledgements

The authors would like to thank the Conselho Nacional de Desenvolvimento Científico e Tecnológico (CNPq), Coordenação de Aperfeiçoamento de Pessoal de Nível Superior (CAPES) and Fundação Carlos Chagas Filho de Amparo à Pesquisa do Estado do Rio de Janeiro (FAPERJ) for their financial support and fellowships.

References

1 B. Wang and S. Dong, *Talanta*, 2000, **51**, 565–572.
2 J. Li, S. N. Tan and J. T. Oh, *J. Electroanal. Chem.*, 1998, **448**, 69–77.
3 W. J. Li, R. Yuan, Y. Q. Chai, L. Zhou, S. H. Chen and L. Li, *J. Biochem. Biophys. Methods*, 2008, **70**, 830–837.

4 J. Li, Q. Liu, Y. Liu, S. Liu and S. Yao, *Anal. Biochem.*, 2005, **346**, 107–117.
5 S. Tan, X. Tan, J. Xu, D. Zhao, J. Zahang and L. Liu, *Anal. Methods*, 2011, **3**, 110–115.
6 J. P. Chen and Y. N. Hwang, *Enzyme Microb. Technol.*, 2003, **33**, 513–519.
7 H. Wu, Y. Liang, J. Shi, X. Wang, D. Yang and Z. Jiang, *Mater. Sci. Eng., C*, 2013, **33**, 1438–1445.
8 J. Singh, M. Srivastava, P. Kalita and B. D. Malhotra, *Process Biochem.*, 2012, **47**, 2189–2198.
9 J.-P. Chen, P.-C. Yang, Y.-H. Ma, S.-J. Tu and Y.-J. Lu, *Int. J. Nanomed.*, 2012, **7**, 5137–5149.
10 A. A. Ansari, G. Sumana, M. K. Pandey and B. D. Malhotra, *J. Mater. Res.*, 2009, **24**, 1667–1673.
11 G. Silveira, A. de Morais, P. C. M. Villis, C. M. Maroneze, Y. Gushikem, A. M. S. Luchoand and F. L. Pissetti, *J. Colloid Interface Sci.*, 2012, **369**, 302–308.
12 E. Marafon, L. T. Kubota and Y. Gushikem, *J. Solid State Electrochem.*, 2009, **13**, 377–383.
13 J. Arguello, V. L. Leidens, H. A. Magosso, R. R. Ramos and Y. Gushikem, *Electrochim. Acta*, 2008, **54**, 560–565.
14 E. S. Ribeiro, S. L. P. Dias, Y. Gushikem and L. T. Kubota, *Electrochim. Acta*, 2004, **49**, 829–834.
15 E. S. Ribeiro, S. L. P. Dias, S. T. Fujiwara, Y. Gushikem and R. E. Bruns, *J. Appl. Electrochem.*, 2003, **33**, 1069–1075.
16 E. S. Ribeiro, Y. Gushikem, J. C. Biazzotto and O. A. Serra, *J. Porphyrins Phthalocyanines*, 2002, **6**, 527–532.
17 G. Zaitseva, Y. Gushikem, E. R. Ribeiro and S. S. Rosatto, *Electrochim. Acta*, 2002, **47**, 1469–1474.
18 A. M. Castellani and Y. Gushikem, *J. Colloid Interface Sci.*, 2000, **230**, 195–199.
19 E. S. Ribeiro, S. S. Rosatto, Y. Gushikem and L. T. Kubota, *Solid State Electrochem.*, 2003, **7**, 665–670.
20 X. T. Gao, J. L. G. Fierro and I. E. Wachs, *Langmuir*, 1999, **15**, 3169–3178.
21 J. E. Gonçalves, Y. Gushikem and S. C. de Castro, *J. Non-Cryst. Solids*, 1999, **260**, 125–131.
22 V. Menon, V. T. Popa, C. Contescu and J. A. Schwarz, *Rev. Roum. Chim.*, 1998, **43**, 393–397.
23 J. M. Miller and L. J. Lakshmi, *J. Phys. Chem. B*, 1998, **102**, 6465–6470.
24 H. Kochkar and F. Figueras, *J. Catal.*, 1997, **171**, 420–430.
25 D. C. M. Dutoit, M. Schneider, P. Fabrizioli and A. Baikerm, *J. Mater. Chem.*, 1997, **7**, 271–278.
26 S. Singh, D. V. S. Jain and M. L. Singla, *Sens. Actuators, B*, 2013, **182**, 161–169.
27 S. Zuo, Y. Teng, H. Yuan and M. Lan, *Sens. Actuators, B*, 2008, **133**, 555–560.
28 V. Singh and D. Singh, *Process Biochem.*, 2013, **48**, 96–102.
29 B. Wang and S. Dong, *J. Electroanal. Chem.*, 2000, **487**, 45–50.
30 C.-H. Lee, T.-S. Lin and C.-Y. Mou, *Nano Today*, 2009, **4**, 165–179.
31 V. B. Kandimalla, V. S. Tripathi and H. Ju, *Electrochemical Sensors, Biosensor and their Biomedical Applications*, 2008, chapter 16, pp. 503–529.
32 X. Chen and S. Dong, *Biosens. Bioelectron.*, 2003, **18**, 999–1004.
33 S. N. Tan, W. Wang and L. Ge, *Comprehensive Biomaterials*, 2011, vol. 3, pp. 471–489.
34 R. Gupta and N. K. Chaudhury, *Biosens. Bioelectron.*, 2007, **22**, 2387–2399.
35 J. Wang, *Anal. Chim. Acta*, 1999, **399**, 21–27.
36 V. G. Gavalas, S. A. Law, J. C. Ball, R. Andrews and L. G. Bachas, *Anal. Biochem.*, 2004, **329**, 247–252.
37 M. Sundaramoorthy, J. Terner and T. L. Poulos, *Structure*, 1995, **3**, 1367–1377.
38 G. Bayramoplu, S. Kiralp, M. Yilmaz, L. Toppare and M. Y. Arica, *Biochem. Eng. J.*, 2008, **38**, 180–188.
39 S. S. Rosatto, P. T. Sotomayor, L. T. Kubota and Y. Gushikem, *Electrochim. Acta*, 2002, **47**, 4451–4458.
40 W. Li, R. Yuan, Y. Chai, L. Zhou, S. Chen and N. Li, *J. Biochem. Biophys. Methods*, 2008, **70**, 830–837.
41 G. Bayramoğlua, S. Kiralpb, M. Yilmaza, L. Toppareb and M. Y. Arıca, *Biochem. Eng. J.*, 2008, **38**, 180–188.
42 G. F. Lima, M. O. Ohara, D. N. Clausen, D. R. Nascimento, E. S. Ribeiro, M. G. Segatelli, M. A. Bezerra and C. R. T. Tarley, *Microchim. Acta*, 2012, **178**, 61–70.
43 L. M. Costa, E. S. Ribeiro, M. G. Segatelli, D. R. do Nascimento, F. M. Oliveira and C. R. T. Tarley, *Spectrochim. Acta, Part B*, 2011, **66**, 329–337.
44 C. R. T. Tarley, T. C. de Avila, M. G. Segatelli, G. D. Lima, G. D. Peregrino, C. W. Scheeren, S. L. P. Dias and E. S. Ribeiro, *J. Braz. Chem. Soc.*, 2010, **21**, 1106–1116.
45 J. P. Marco, K. B. Borges, C. R. T. Tarley, E. S. Ribeiro and A. C. Pereira, *J. Electroanal. Chem.*, 2013, **704**, 159–168.
46 J. P. Marco, K. B. Borges, C. R. T. Tarley, E. S. Ribeiro and A. C. Pereira, *Sens. Actuators, B*, 2013, **177**, 251–259.
47 H. Yoshida, N. Matsushita, Y. Kato and T. Hattori, *J. Phys. Chem. B*, 2003, **107**, 8355–8362.
48 M. Crisan, M. Zaharescu, A. Jitianu, D. Crisan and M. Preda, *J. Sol-Gel Sci. Technol.*, 2000, **19**, 409–412.
49 N. Economidis, R. F. Coil and P. G. Smirniotis, *Catal. Today*, 1998, **40**, 27–37.
50 F. D'Acapito, S. Mobilio, P. Gastaldo, D. Barbier, L. F. Santos, O. Martins and R. M. Almeida, *J. Non-Cryst. Solids*, 2001, **293**, 118–124.
51 J. A. Melero, R. Van Grieken, D. P. Serrano and J. J. Espada, *J. Mater. Chem.*, 2001, **11**, 519–1525.
52 D. L. Massart, *Handbook of chemometrics and qualimetrics: part A.*, 1997, Elsevier, New York.
53 J. C. Miller and J. N. Miller, *Statistics for analytical chemistry*. Prentice Hall, 1993, New York.
54 T. R. T. A. Antonio, M. F. Cabral, I. Cesarino, S. A. S. Machado and V. A. Pedrosa, *Electrochem. Commun.*, 2013, **29**, 41–44.
55 R. W. Gerlach, H. L. Tucker, M. K. Anastasia and M. L. Barker, *Compendium of Continuing Education in Dentistry*, 2005, **26**, 874–878.
56 S. Palanisamy, S. Cheemalapati and S. M. Chen, *Anal. Biochem.*, 2012, **429**, 108–115.

57 F. C. Wang, R. Yuan and Y. Q. Chai, *Eur. Food Res. Technol.*, 2007, **225**, 95–104.
58 Y. H. Lin, X. L. Cui and L. Y. Li, *Electrochem. Commun.*, 2005, **7**, 166–172.
59 X. L. Wang, H. Zhang, E. B. Wang, Z. B. Han and C. W. Hu, *Mater. Lett.*, 2004, **58**, 1661–1664.
60 Y. D. Zhao, Y. H. Bi, W. D. Zhang, Q. M. Lu, V. M. Ivama and S. H. P. Serrano, *J. Braz. Chem. Soc.*, 2003, **14**, 551–555.